CMS Physics Analysis Summary

Contact: cms-pag-conveners-exotica@cern.ch 2024/06/04

Search for a neutral gauge boson with non-universal fermion couplings in vector boson fusion processes in proton-proton collisions at $\sqrt{s} = 13$ TeV

The CMS Collaboration

Abstract

The first search for a heavy neutral spin-1 gauge boson (Z') produced via vector boson fusion processes is presented. The analysis considers scenarios in which the Z' boson has non-universal fermion couplings, favoring higher-generation fermions. This offers a new physics phase space not yet fully explored at the LHC. The analysis is performed using LHC data at $\sqrt{s} = 13$ TeV, collected from 2016 to 2018, corresponding to an integrated luminosity of 138 fb^{-1}. The data are consistent with the standard model expectation. Upper limits are set on the product of the Z' cross section and the branching fraction for a Z' boson decaying to $\tau\tau$ or WW. Masses below 2.45 TeV are excluded, depending on the Z' coupling to weak bosons.

The standard model (SM) of particle physics has been a successful theory to explain many experimental observations. However, it is not an ultimate theory of nature. For example, the SM fails to explain neutrino masses, matter-antimatter asymmetry, and the particle nature of dark matter. Furthermore, recent experimental results from precision measurements regarding the decay ratios of B mesons [1–11] and the measurement of the muon anomalous magnetic moment [12] show significant deviations from the SM expectation [13]. Various models of physics beyond the SM (BSM) have been proposed to address these shortcomings. Examples of such models include minimal $\mathrm{U}(1)_X$ extensions [14], top-assisted technicolor models [15], Randall-Sundrum models [16–18], grand unified theories [19], and $E(6)$ models [20]. Such models predict new heavy neutral gauge bosons, referred to as Z′, that could be observed in proton-proton (pp) collisions at the CERN LHC.

The existence of Z′ bosons has been extensively probed at the LHC, mainly considering production via Drell-Yan processes with sizable Z′ coupling (g_q) to light quarks [21–28]. A widely-used benchmark model in those searches is the sequential SM (SSM), which assumes a Z′ boson with the same couplings to quarks and leptons as the SM Z boson. Although $\mathrm{Z}'_{\mathrm{SSM}}$ masses have been excluded by the ATLAS and CMS Collaborations for masses up to 5 TeV, considering Z′ decays to electron and muon pairs, the bounds on $m(\mathrm{Z}')$ are significantly weaker under different assumptions (e.g., non-universal fermion couplings, NUFC) [29, 30]. Furthermore, the lack of evidence in current searches point to Z′ having different features, e.g., small g_q, from what is traditionally assumed, thus remaining concealed in processes not yet investigated. This analysis focused on BSM scenarios with a Z′ boson that couples with strength κ_V to the SM weak bosons and has NUFC. These models motivate a search for Z′ resonances produced via interactions with SM weak bosons, and where the Z′ decays to a pair of τ leptons. Such a pattern with NUFCs can explain the current tensions with the SM observed in the muon $g-2$ results and the anomalies in the B meson sector.

This note presents the first search for a Z′ boson considering production through vector boson fusion (VBF) processes at the LHC, using 138 fb^{-1} of data collected during 2016-2018 from pp collisions at $\sqrt{s} = 13\,\mathrm{TeV}$. In a VBF reaction a quark from each of the colliding protons radiates an SM electroweak vector boson, and the merger of these produces a Z′ boson. The subsequent decay of the Z′ boson leads to a pair of τ leptons or of W bosons, which are accompanied by two jets from the scattered quarks. Four Z′ decay channels are utilized: $\mathrm{e}\mu$, $\mu\tau_\mathrm{h}$, $\mathrm{e}\tau_\mathrm{h}$, and $\tau_\mathrm{h}\tau_\mathrm{h}$, where τ_h refers to a τ lepton that decays hadronically. In the $\mathrm{Z}' \to \tau^+\tau^-$ mode, the electrons and muons are produced from the leptonic decays of τ leptons, while they may arise directly from $\mathrm{W} \to \ell\nu$ decays in the case of the $\mathrm{Z}' \to \mathrm{W}^+\mathrm{W}^-$ mode.

The central feature of the CMS detector is its superconducting solenoid magnet with 6 m inner diameter, which provides magnetic field of 3.8 T. Inside this solenoid magnet, there are three sub-detectors: a silicon pixel and strip tracker, a lead tungstate crystal electromagnetic calorimeter (ECAL), and a brass and scintillator hadron calorimeter (HCAL) composed of a barrel and two endcap sections. Outside the solenoid magnet, an iron quartz fiber hadron calorimeter is placed in the forward region (at pseudorapidity $3 < |\eta| < 5$) of the CMS detector to detect forward particles. Muon detectors are embedded in the iron flux-return yoke surrounding the solenoid magnet to measure the momentum of muons. A detailed description of the CMS detector can be found in [31].

Events are reconstructed from particle candidates (electrons, muons, photons, and hadrons) identified using the particle-flow (PF) algorithm [32]. The algorithm combines information from all sub-detectors to classify final-state particles produced in the collision. The resulting set of particles is used to reconstruct the τ_h candidates, jets, missing transverse momentum, and

the isolation variables described below. The primary vertex (PV) is taken to be the vertex corresponding to the hardest scattering in the event, evaluated using tracking information alone, as described in Section 9.4.1 of Ref. [33]. Electron candidates are reconstructed by matching energy clusters in the ECAL with tracks in the inner tracker. A dedicated electron identification is used to distinguish electrons produced in hard scattering processes from charged hadrons and from electrons produced through photon conversions [34]. Muons are reconstructed using the tracker and muon chambers and by requiring consistency with low-energy measurements in the calorimeters. The electron and muon selections impose an isolation requirement to suppress both jets erroneously identified as leptons and genuine leptons from hadron decays. The isolation variable I_ℓ is defined as the scalar p_T sum, divided by the lepton p_T, of charged and neutral PF candidates within a cone in $(\eta, \phi$, with ϕ the azimuthal angle) of radius 0.4 (0.3) around the muon (electron) direction at the interaction vertex. The sum excludes the lepton under consideration as well as particles identified as arising from additional pp interactions within the same or a nearby bunch crossing ("pileup"). The isolation criterion is $I_\ell < 0.15$ [35].

Jets are clustered using the anti-k_T clustering algorithm [36, 37] with a distance parameter of 0.4. Identification criteria are applied to jet candidates to remove anomalous effects from the calorimeters [38]. For jets with $p_T > 30\,\text{GeV}$, the identification efficiency is >90% depending on pseudorapidity. The jet energy scale and resolution are corrected depending on the p_T and η of the jet [39]. Jets originating from the hadronization of b quarks are identified using secondary vertexing algorithms. The identification efficiency is 40–60% for genuine b jets, depending on p_T, η, and the year of data collection, and the light-flavor quark or gluon misidentification rate is 0.1–0.9% [40].

Hadronic decays of τ leptons are reconstructed and differentiated from light-flavor quark and gluon jets using the hadrons-plus-strips algorithm [41] and are identified using a discriminator based on a neural network that combines variables related to isolation and the τ lepton lifetime to identify specific classes of τ_h decay modes [42]. The tight-isolation working point is used to define the signal region, which results in a τ_h identification efficiency of 60% for this analysis, and a 0.05-0.3% probability for a jet to be misidentified as a τ_h, depending on the p_T and η values of the τ_h candidate [42]. The loose-isolation working point, which is used for background estimation studies, has a τ_h identification efficiency of 80% and a 0.1-1% jet misidentification probability. To discriminate τ_h from muons and electrons, a neural network based lepton rejection discriminator is used that requires that the lead track of the τ_h not be associated with a global muon signature or an electron bremsstrahlung shower [43]. The misidentification rate for electrons (muons) is 3.60 (0.02)% for a genuine τ_h identification efficiency of 80%.

The missing transverse momentum $\vec{p}_T^{\,\text{miss}}$ is the negative vector p_T sum of all PF candidates. Its magnitude is p_T^{miss}. Production of undetected particles such as SM neutrinos is inferred from the measured p_T^{miss} [44, 45]. The jet corrections described are propagated as corrections to p_T^{miss}, which improves the agreement in p_T^{miss} between simulation and data.

Data for this search were collected using single-lepton triggers for final states with electrons or muons, and a double-τ_h trigger for the $\tau_h\tau_h$ analysis [46]. The single muon (electron) trigger requires an isolated muon (electron) with a minimum p_T of 24 or 27 GeV (32 or 35 GeV), depending on the year. The double-τ_h trigger uses isolation criteria and $p_T(\tau_h)$ thresholds of 32, 35, or 40 GeV, depending on the year.

Events satisfying the trigger selections must pass additional offline lepton requirements. An event must contain exactly one pair of leptons having opposite electric charge (OS). The muon in the eμ ($\mu\tau_h$) channel is required to have $p_T > 30\,(35)\,\text{GeV}$ within $|\eta| < 2.1$. The electron in the eμ (eτ_h) channel is required to have $p_T > 10\,(55)\,\text{GeV}$ within $|\eta| < 2.1$. The τ_h candidates

in the $\tau_h\tau_h$ ($\mu\tau_h$ & $e\tau_h$) channel are required to have $p_T > 70\,(20)$ GeV within $|\eta| < 2.1$, where the trigger is fully efficient.

Experimentally, the distinctive signature of events resulting from VBF processes is the presence of two energetic jets with a large η separation ($\Delta\eta$), located in opposite hemispheres of the CMS detector ($\eta_{j1}\eta_{j2} < 0$). Therefore, in addition to the criteria of a lepton pair targeting the $Z' \to \tau^+\tau^-$ and $Z' \to W^+W^-$ decay chains, we require two well-identified jets with $p_T > 30$ GeV and $|\eta| < 5$, with reconstructed dijet mass (m_{jj}) above 500 GeV and $|\Delta\eta(jj)| > 4.2$, that fulfill the $\eta_{j1}\eta_{j2} < 0$ requirement. We refer to these requirements as the VBF selections. All selected particle candidates must be well separated from each other by a requirement $\Delta R \equiv \sqrt{(\Delta\eta^2 + \Delta\phi^2)} > 0.4$. To reduce background contamination from SM processes containing t quarks, events must contain no jet with $p_T > 30$ GeV and $|\eta| < 2.4$ identified as a b quark jet. The associated neutrinos from the τ lepton and W boson decays generate sizable p_T^{miss}. We require $p_T^{miss} > 30$ GeV to suppress the contribution from quantum chromodynamic processes (QCD multijet events). We use the reconstructed mass between the two lepton candidates and $\vec{p}_T^{miss}$, $m(\ell_1, \ell_2, p_T^{miss})$, as the main observable to search for the presence of signal among background events. The reconstructed mass is defined as $m(\ell_1, \ell_2, p_T^{miss}) = \sqrt{(E_{\ell_1} + E_{\ell_2} + p_T^{miss})^2 - (\vec{p}_{\ell_1} + \vec{p}_{\ell_2} + \vec{p}_T^{miss})^2}$. The $m(\ell_1, \ell_2, p_T^{miss})$ in signal events probes the Z' mass scale, and is expected to be larger on average than for the backgrounds. The strategy is to search for a broad enhancement in the large $m(\ell_1, \ell_2, p_T^{miss})$ part of the spectrum.

The dominant SM background processes contributing to the search are W and Z boson production in association with jets (W+jets and Z+jets), t quark pairs, and QCD multijet. The W+jets and Z+jets events contain genuine lepton candidates, energetic jets, and p_T^{miss} from neutrinos. Background from t quark pairs ($t\bar{t}$) events is characterized by two b quark jets in addition to genuine leptons. QCD multijet events arise from jets misidentified as leptons.

Simulated samples for Z+jets, W+jets, and single-t-quark events are produced with the MADGRAPH5_aMC@NLO 2.6.0 program [47] at leading order (LO) in QCD. Events from $t\bar{t}$ plus jets are generated with POWHEG 2.0 [48] at next-to-leading order (NLO) accuracy [48]. The LO PYTHIA generator [49] is used to model diboson (VV) processes. The signal samples are generated using MADGRAPH5_aMC@NLO at LO accuracy, considering the production of a Z' and two associated jets ($pp \to Z'jj$), with the QCD vertex suppressed to isolate events from pure electroweak processes. At the MADGRAPH5_aMC@NLO parton level, jets have $p_T > 20$ GeV and $|\eta| < 5.0$. Furthermore, the jet pair must be separated in η-ϕ space, $|\Delta\eta(j_1, j_2)| > 4.2$, and have $m_{jj} > 500$ GeV, to suppress $pp \to VZ' \to jjZ'$ from hadronically decaying W or Z bosons. We use the simplified model in Ref. [50], where the Z' masses and couplings to the SM particles are free parameters. The Z' coupling to first and second generation fermions is defined as $g_\ell g_{Zf\bar{f}}$, where $g_{Zf\bar{f}}$ is the SM Z boson coupling, and g_ℓ is a "modifier" for the coupling. The coupling to third-generation fermions is similarly defined with g_h as the modifier for the SM Z boson coupling to third-generation fermions. Finally, the Z' coupling to the SM weak vector bosons is defined as $g_{Z'VV} = \kappa_V g_{ZVV}$, where g_{ZVV} is the SM Z boson coupling to the SM weak vector bosons and κ_V is a modifier for that coupling. Four sets of signal models are utilized: (*i*) $Z' \to \tau^+\tau^-$ decays with $g_\ell = 0$, henceforth referred to as simplified phenomenological model 1 (SPM1); (*ii*) $Z' \to \tau^+\tau^-$ decays with $g_\ell = 1$ (SPM2); (*iii*) $Z' \to WW$ decays with $g_\ell = 0$ (SPM3); and (*iv*) $Z' \to WW$ decays with $g_\ell = 1$ (SPM4). The $g_\ell = 0$ cases are a proxy for NUFC scenarios, where the couplings of the Z' to light fermions are suppressed. The $g_\ell = 1$ case allows for non-negligible couplings to light fermions. For all sets of signal models described above, five κ_V values are considered: $\kappa_V = 0.1, 0.25, 0.50, 0.75, 1.0$.

The MADGRAPH5_aMC@NLO and POWHEG generators used to simulate signal and background processes are interfaced with PYTHIA 8.212 (and 8.230) using the CUETP8M1 (and CP5 tunes) [51, 52] for parton shower and fragmentation in the 2016 (and 2017-2018) simulated samples, respectively. The NNPDF3.0 LO and NLO [53] parton distribution functions (PDFs) are used in the event generation. The simulated background yields are normalized to the integrated luminosity using next-to-NLO (NNLO) or NLO cross sections in QCD, while signal production cross sections are calculated at LO accuracy. The response of the CMS detector in these Monte Carlo (MC) samples is simulated using dedicated software based on the GEANT4 toolkit [54]. Pileup is incorporated by simulating additional interactions that are both in time and out of time with the collision.

The strategy for the estimation of the background contributions in the signal region (SR) depends on the channel. Where possible, we derive the background with τ_h candidates arising from misidentification of other objects ("misID τ_h"), using data-driven techniques. These make use of τ_h candidates ("antiISO τ_h") that satisfy the loose-, but fail the tight-isolation τ_h identification. The estimation of backgrounds with genuine leptons makes use of simulation combined with data-to-simulation correction factors derived from dedicated control regions (CRs). Small background contributions in the SRs are taken directly from simulation.

For the $e\tau_h$ and $\mu\tau_h$ channels, the main contributing background is from events with jets misidentified as τ_h candidates, mainly coming from processes such as $W+$jets and $t\bar{t}$ with one leptonic W decay. This background contribution is estimated from data using CRs obtained with no VBF selections and containing an antiISO τ_h. Events in this CR are reweighted with two factors: (*i*) a VBF efficiency factor; and (*ii*) a transfer factor, referred to as the misID ratio defined as the ratio of events with nominal τ_h candidates to events with an antiISO τ_h. The misID ratios are derived as a function of $p_T(\tau_h)$ and $\eta(\tau_h)$ in a $Z(\to\mu\mu)+\tau_h$ CR, where the τ_h is a misidentified jet. The VBF efficiency is calculated from data, using a $W(\to\mu\nu)+$jets CR with transverse mass $m_T(\vec{p}_\mu, \vec{p}_T^{\,miss})$ near the Jacobian m_W peak. The measurements between data and simulation agree within statistical uncertainties. Any residual $m(\ell_1, \ell_2, p_T^{miss})$ shape biases in the misID τ_h background prediction are accounted for using correction factors, as a function of $\Delta\phi(\vec{p}_\ell, \vec{p}_T^{\,miss})$, derived from the MC samples.

The dominant genuine-τ_h background contribution in the $e\tau_h$ and $\mu\tau_h$ SRs arises from $t\bar{t}$ fully-leptonic events. This background is estimated using data-to-simulation efficiency scale factors (SFs), implemented to account for differences between the data and the modeling of the selection efficiencies in simulation. The SFs are measured in dedicated CRs requiring the same lepton pair criteria as for the SR, but, in addition, selecting events with one b jet candidate. Events are divided into two categories: (1) passing nominal VBF selections; and (2) failing the VBF criteria. The CR composed of events failing the VBF criteria serves to calibrate the modeling of the non-VBF selections in simulation. The CR with events satisfying the VBF criteria allows us to measure the SFs associated with the modeling of the VBF efficiency.

For the $\tau_h\tau_h$ channel, the main contribution comes from $Z+$jets processes with genuine τ_h candidates, and is estimated from simulation using SFs obtained from dedicated CRs. The CRs are obtained using the same selection criteria for the lepton pair as in the SR, but requiring the reconstructed mass $m(\tau_h\tau_h)$ of the two τ_h candidates to be between 50 and 100 GeV, the peak range for $Z \to \tau_h\tau_h$. Events passing these requirements are used to measure one SF to determine the data-to-MC agreement associated with the modeling of τ_h candidates, while events additionally satisfying the VBF criteria are used to obtain a second SF to measure the level of agreement between data and simulation associated with the VBF dijet efficiency. The contribution of QCD multijet events in these $Z(\to\tau_h\tau_h)+$jets CRs is estimated from data using

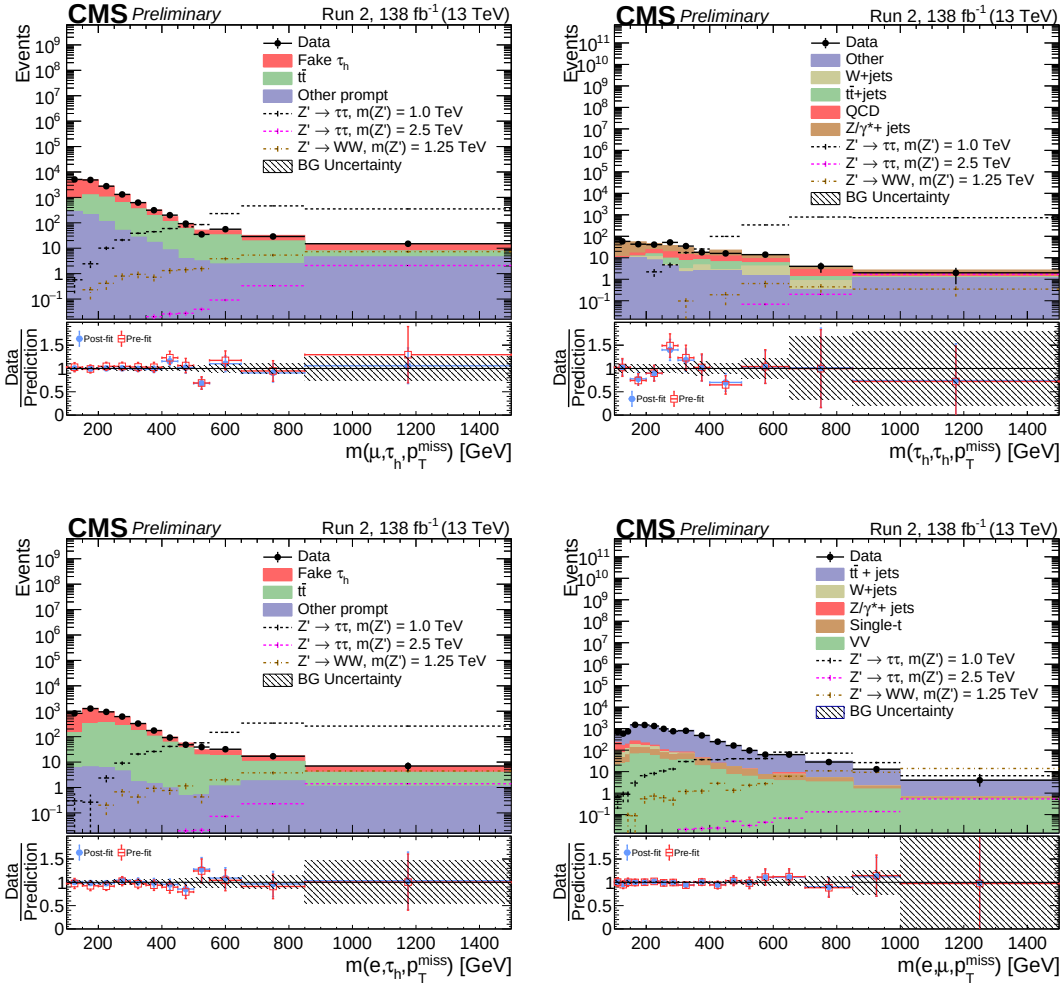

Figure 1: Observed $m(\ell_1, \ell_2, p_{\mathrm{T}}^{\mathrm{miss}})$ for the data, and the post-fit backgrounds (stacked histograms), in the signal region for $\mu\tau_{\mathrm{h}}$ (upper left), $\tau_{\mathrm{h}}\tau_{\mathrm{h}}$ (upper right), $\mathrm{e}\tau_{\mathrm{h}}$ (lower left), and $\mathrm{e}\mu$ (lower right) channels. The lower panels show ratios of the data to the pre-fit background prediction and post-fit background yield as red open squares and blue points, respectively. The gray band in the lower panels indicates the systematic component of the post-fit uncertainty. The dashed lines correspond to the signal expectation, for Z′ masses of 1 TeV (black) and 2.5 TeV (magenta) decaying to $\tau^+\tau^-$, normalized to 199.4 fb and 0.7504 fb respectively. The dashed brown line corresponds to Z′ mass of 1.25 TeV decaying to $\mathrm{W}^+\mathrm{W}^-$, normalized to 61.14 fb.

CRs obtained with τ_{h} pairs having the same electric charge (LS). The transfer factor between LS and OS events is calculated using events with antiISO τ_{h} and $m(\tau_{\mathrm{h}}\tau_{\mathrm{h}}) > 100\,\mathrm{GeV}$. Correction factors of 0.96 ± 0.2, 0.95 ± 0.16, and 1.17 ± 0.16 for $\mathrm{Z}(\to\tau_{\mathrm{h}}\tau_{\mathrm{h}})+$jets are measured in this CR for the 2016, 2017, and 2018 data sets, respectively. The uncertainties are purely statistical. These correction factors are used to scale the $\mathrm{Z}(\to\tau^+\tau^-)+$jets prediction in the SR.

The contribution of QCD multijet events in the $\tau_{\mathrm{h}}\tau_{\mathrm{h}}$ SR is determined using data. An enriched CR with QCD multijet events is obtained by the requirement of an LS τ_{h} pair. This CR is used to obtain the expected yield of QCD multijet events in the SR. The expected QCD SR yield is estimated using as a transfer factor the ratio of OS to LS τ_{h} pairs, using two different CRs. These CRs are obtained by selecting events that fail the VBF and $p_{\mathrm{T}}^{\mathrm{miss}}$ criteria and have either an OS or an LS antiISO τ_{h} pair. The smaller W+jets background contribution in the $\tau_{\mathrm{h}}\tau_{\mathrm{h}}$ SR is

determined by correcting the prediction from simulation with VBF and non-VBF efficiency SFs derived from high-purity $\mathrm{W}(\to\mu\nu)+$ jets control samples.

In the $\mathrm{e}\mu$ channel, the main contribution comes from the $\mathrm{t\bar{t}}$ background, with fully leptonic t quark decays. A data-driven estimation of the $\mathrm{t\bar{t}}$ background is performed using the classic *ABCD* method, in which region *A* is the SR, and regions *B*, *C*, and *D* are defined by selections similar to those if the SR, but with one or two modifications to insure that all four regions are orthogonal. CR*B* is defined with events containing exactly one b jet candidate, CR*C* with events containing one b jet candidate and failing the VBF criteria, and CR*D* with the same b jet veto as the SR but failing the VBF criteria. The $\mathrm{t\bar{t}}$ yield N_A in the SR for each $m(\mathrm{e},\mu,p_{\mathrm{T}}^{\mathrm{miss}})$ bin is obtained as $N_A = (N_B/N_C)N_D$, where N_B and N_C are the data yields in those respective CRs, and N_D is given by the yield in CR*D* minus an estimate from simulation of the contribution of non-$\mathrm{t\bar{t}}$ processes. Closure tests for this methodology are performed using simulation, and additional tests are carried out using data CRs with two b jet candidates.

Various effects impact the predicted shape and normalization of the reconstructed $m(\ell_1,\ell_2,p_{\mathrm{T}}^{\mathrm{miss}})$ background distribution. The major source of systematic uncertainty comes from the difference in the misID τ_{h} ratios between light quark and gluon jets. This uncertainty is determined by the deviation of the misID ratios obtained in a $\mathrm{Z}(\to\mu\mu)+\tau_{\mathrm{h}}$ sample, where the τ_{h} is a misidentified jet, from those in a sample of $\mathrm{W}(\to\mu\nu)+\tau_{\mathrm{h}}$ events with a like-sign $\mu\tau_{\mathrm{h}}$ pair. This uncertainty depends on $p_{\mathrm{T}}(\tau_{\mathrm{h}})$ and varies from 4 to 20%. Uncertainties of 1–21%, depending on the process, in the background predictions arise from the statistical uncertainties of the data in the CRs used for measuring SFs. Another source of systematic uncertainty is the closure of the background estimation methods, where closure refers to tests made (on data and simulation) to check that the background determination techniques reproduce the expected background distributions in both rate and shape within the statistical uncertainties. The background estimation uncertainty from the closure tests is <20% for all processes.

The signal and background yields estimated from simulation are affected by similar sources of systematic uncertainty, with small differences between the 2016, 2017, and 2018 data sets. The integrated luminosities for the 2016, 2017, and 2018 data-taking years have 1.2–2.5% individual uncertainties [55–57], while the overall uncertainty for the 2016–2018 period is 1.6%. Uncertainties due to the identification of μ and e are <1% for all background and signal processes [34, 58, 59]. The uncertainty from the τ_{h} identification and isolation requirements is 6–9%, depending on the year. The uncertainty on the τ_{h} energy scale amounts to 2%. For the electrons misidentified as τ_{h} candidates, the uncertainties are 1–6.5% depending on the $p_{\mathrm{T}}(\tau_{\mathrm{h}})$. The jet energy scale uncertainties (2–5% depending on η and $p_{\mathrm{T}}^{\mathrm{miss}}$) result in an uncertainty of 1–3% depending on $m(\ell_1,\ell_2,p_{\mathrm{T}}^{\mathrm{miss}})$. The uncertainty in event acceptance from the PDF set used in simulation is determined according to the PDF4LHC recommendations [60] by comparing the outputs from CTEQ6.6L, MSTW08, and NNPDF10 PDF sets [61–63] to those of the default PDF set. This results in at most a 6% uncertainty for the signal processes, and for the background processes that are derived entirely from simulation. The uncertainty in the b tagging efficiency results in 2–9% uncertainty on the predicted yields, depending on the process. The trigger uncertainty is 3% for background and signal. During the 2016 and 2017 data-taking, a gradual shift in the timing of the inputs of the ECAL L1 trigger in the region at $|\eta| > 2.0$ caused a specific trigger inefficiency. For events containing an electron (a jet) with p_{T} larger than ≈50 GeV (≈100 GeV), in the region $2.5 < |\eta| < 3.0$ the efficiency loss is ≈10–20%, depending on p_{T}, η, and time. Correction factors were computed from data and applied to the acceptance evaluated by simulation.

Figure 1 shows the $m(\ell_1,\ell_2,p_{\mathrm{T}}^{\mathrm{miss}})$ distribution for events in the SRs for all channels. The bin-

ning was chosen to optimize for discovery potential. The observed mass spectra shown in Fig. 1 are consistent with the SM predictions. We therefore set 95% confidence level (CL) upper limits on the product of the VBF Z′ cross section and the branching fraction for the decay of the Z′ boson to $\tau^+\tau^-$ or W^+W^-. The limits are estimated following the modified frequentist construction CL_s using the CMS statistical analysis tool COMBINE [64–67]. Maximum likelihood fits are performed using the observed distributions to construct a combined profile likelihood ratio test statistic in bins of $m(\ell_1, \ell_2, p_T^{miss})$. Systematic uncertainties are implemented as nuisance parameters, which are profiled and modeled with gamma or log-normal priors for normalization parameters and Gaussian priors for shape uncertainties.

Figure 2 shows exclusion bounds for the four signal models described above, as a function of $m(Z')$ and the $Z' \to \tau^+\tau^-$ and $Z' \to W^+W^-$ branching fractions, assuming different κ_V values.

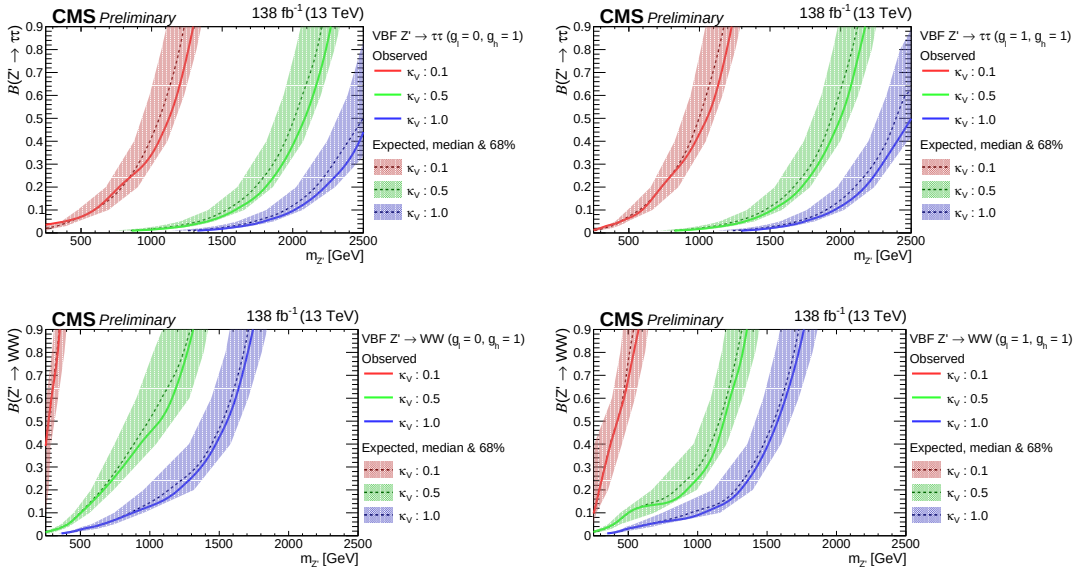

Figure 2: Combined 95% CL upper limits on $m(Z')$ as a function of Z′ branching fraction to $\tau^+\tau^-$ for the $g_\ell = 0$ scenario (upper left), $\tau^+\tau^-$ for the $g_\ell = 1$ scenario (upper right), W^+W^- for the $g_\ell = 0$ scenario (lower left), and W^+W^- for the $g_\ell = 1$ scenario (lower right). The red, green and blue curves correspond to κ_V equal to 0.1, 0.5 and 1 respectively.

Due to the high branching fraction to hadronic decays, the $\tau_h\tau_h$ channel contributes the most to the $Z' \to \tau^+\tau^-$ exclusion limits. There is no significant difference in impact between the semi-leptonic τ pair decay channels. The situation inverts for the $Z' \to W^+W^-$ with the $e\mu$ channel contributing the most to this type of exclusion. For SPM1, the data exclude Z′ bosons with masses below 1 (2.45) TeV for a $Z' \to \tau^+\tau^-$ branching fraction of 50%, assuming $\kappa_V = 0.1$ (1.0). For SPM2, the bounds on $m(Z')$ increase by about 5% due to an increase in the $pp \to Z'jj$ cross section (from pure electroweak non-VBF processes) when $g_\ell = 1$. For SPM3 and SPM4, we exclude Z′ with masses below about 1.6 TeV for a 50% $Z' \to W^+W^-$ branching fraction, assuming $\kappa_V = 1.0$.

In summary, a search for a heavy neutral spin-1 gauge boson (Z′) produced via vector boson fusion processes has been performed for the first time using data collected by the CMS experiment, corresponding to an integrated luminosity of 138 fb^{-1}. This is the first ever search for Z′ produced through vector boson fusion performed at the LHC. The search considers non-universal couplings (NUC) of Z′ bosons to fermions, including scenarios with dominant couplings to third-generation fermions. Theoretical models aiming to explain B−meson anoma-

lies in the R_{D^*} ratios [68–73] often include associated production of Z' and W' bosons with NUC [74, 75]. Therefore, this search serves as an indirect probe to bound the available phase space for these models. Two decay channels, $Z' \to \tau^+\tau^-$ and $Z' \to W^+W^-$, are considered, motivated by recent anomalies in the precision measurements of B meson decays. The invariant mass of the dilepton plus missing transverse momentum is used to search for the presence of signal as a broad enhancement above the background expectation. The data do not reveal evidence for new physics. In Z' models with non-universal fermion couplings, in particular models with Z' bosons that exhibit enhanced couplings to third-generation fermions, the presence of Z' bosons decaying to a tau lepton (W boson) pair is excluded for Z' masses up to 2.45 TeV (1.5 TeV), depending on the Z' coupling to SM weak bosons, resulting in the most stringent limits on these models to date.

References

[1] Belle Collaboration, "Measurement of the Differential Branching Fraction and Forward-Backward Asymmetry for $B \to K^{(*)}\ell^+\ell^-$", *Phys. Rev. Lett.* **103** (2009) 171801, doi:10.1103/PhysRevLett.103.171801, arXiv:0904.0770.

[2] Belle Collaboration, A. Abdesselam et al., "Angular analysis of $B^0 \to K^*(892)^0\ell^+\ell^-$", in *LHC Ski 2016: A First Discussion of 13 TeV Results*. 2016. arXiv:1604.04042.

[3] Belle Collaboration, "Lepton-Flavor-Dependent Angular Analysis of $B \to K^*\ell^+\ell^-$", *Phys. Rev. Lett.* **118** (2017), no. 11, 111801, doi:10.1103/PhysRevLett.118.111801, arXiv:1612.05014.

[4] BaBar Collaboration, "Measurements of branching fractions, rate asymmetries, and angular distributions in the rare decays $B \to K\ell^+\ell^-$ and $B \to K^*\ell^+\ell^-$", *Phys. Rev. D* **73** (2006) 092001, doi:10.1103/PhysRevD.73.092001, arXiv:hep-ex/0604007.

[5] BaBar Collaboration, "Measurement of angular asymmetries in the decays $B \to K^*\ell^+\ell^-$", *Phys. Rev. D* **93** (2016), no. 5, 052015, doi:10.1103/PhysRevD.93.052015, arXiv:1508.07960.

[6] LHCb Collaboration, "Differential branching fractions and isospin asymmetries of $B \to K^{(*)}\mu^+\mu^-$ decays", *JHEP* **06** (2014) 133, doi:10.1007/JHEP06(2014)133, arXiv:1403.8044.

[7] LHCb Collaboration, "Angular analysis and differential branching fraction of the decay $B_s^0 \to \phi\mu^+\mu^-$", *JHEP* **09** (2015) 179, doi:10.1007/JHEP09(2015)179, arXiv:1506.08777.

[8] LHCb Collaboration, "Measurements of the S-wave fraction in $B^0 \to K^+\pi^-\mu^+\mu^-$ decays and the $B^0 \to K^*(892)^0\mu^+\mu^-$ differential branching fraction", *JHEP* **11** (2016) 047, doi:10.1007/JHEP11(2016)047, arXiv:1606.04731. [Erratum: JHEP 04, 142 (2017)].

[9] LHCb Collaboration, "Search for lepton-universality violation in $B^+ \to K^+\ell^+\ell^-$ decays", *Phys. Rev. Lett.* **122** (2019), no. 19, 191801, doi:10.1103/PhysRevLett.122.191801, arXiv:1903.09252.

[10] LHCb Collaboration, "Test of lepton universality in beauty-quark decays", *Nature Phys.* **18** (2022) 277, doi:10.1038/s41567-021-01478-8, arXiv:2103.11769.

[11] LHCb Collaboration, "Measurement of lepton universality parameters in $B^+ \to K^+\ell^+\ell^-$ and $B^0 \to K^{*0}\ell^+\ell^-$ decays", *Phys. Rev. D* **108** (2023) 032002, doi:10.1103/PhysRevD.108.032002, arXiv:2212.09153.

[12] Muon $g-2$ Collaboration, "Measurement of the positive muon anomalous magnetic moment to 0.46 ppm", *Phys. Rev. Lett.* **126** (2021) 141801, doi:10.1103/PhysRevLett.126.141801.

[13] W. Altmannshofer and P. Stangl, "New physics in rare B decays after Moriond 2021", *Eur. Phys. J. C* **81** (2021), no. 10, 952, doi:10.1140/epjc/s10052-021-09725-1, arXiv:2103.13370.

[14] A. Das, P. S. B. Dev, Y. Hosotani, and S. Mandal, "Probing the minimal U(1)X model at future electron-positron colliders via fermion pair-production channels", *Phys. Rev. D* **105** (2022), no. 11, 115030, doi:10.1103/PhysRevD.105.115030, arXiv:2104.10902.

[15] C. T. Hill, "Topcolor assisted technicolor", *Physics Letters B* **345** (1995), no. 4, 483, doi:10.1016/0370-2693(94)01660-5.

[16] L. Randall and R. Sundrum, "A Large mass hierarchy from a small extra dimension", *Phys. Rev. Lett.* **83** (1999) 3370, doi:10.1103/PhysRevLett.83.3370, arXiv:hep-ph/9905221.

[17] L. Randall and R. Sundrum, "An alternative to compactification", *Physical Review Letters* **83** (1999), no. 23, 4690, doi:10.1103/physrevlett.83.4690.

[18] H. Davoudiasl, J. L. Hewett, and T. G. Rizzo, "Experimental probes of localized gravity: On and off the wall", *Phys. Rev. D* **63** (2001) 075004, doi:10.1103/PhysRevD.63.075004, arXiv:hep-ph/0006041.

[19] P. K. Mohapatra, R. N. Mohapatra, and P. B. Pal, "Implications of $e(6)$ grand unification", *Phys. Rev. D* **33** (1986) 2010, doi:10.1103/PhysRevD.33.2010.

[20] D. London and J. L. Rosner, "Extra gauge bosons in $e(6)$", *Phys. Rev. D* **34** (1986) 1530, doi:10.1103/PhysRevD.34.1530.

[21] CMS Collaboration, "Search for resonant and nonresonant new phenomena in high-mass dilepton final states at $\sqrt{s}$ = 13 tev", *JHEP* **07** (2021) 208, doi:10.1007/JHEP07(2021)208, arXiv:2103.02708.

[22] CMS Collaboration, "Search for heavy resonances decaying to tau lepton pairs in proton-proton collisions at $\sqrt{s} = 13$ TeV", *JHEP* **02** (2017) 048, doi:10.1007/JHEP02(2017)048, arXiv:1611.06594.

[23] CMS Collaboration, "Search for High-Mass Resonances Decaying into τ-Lepton Pairs in pp Collisions at $\sqrt{s} = 7$ TeV", *Phys. Lett. B* **716** (2012) 82, doi:10.1016/j.physletb.2012.07.062, arXiv:1206.1725.

[24] CMS Collaboration, "Search for Heavy Narrow Dilepton Resonances in pp Collisions at $\sqrt{s} = 7$ TeV and $\sqrt{s} = 8$ TeV", *Phys. Lett. B* **720** (2013) 63, doi:10.1016/j.physletb.2013.02.003, arXiv:1212.6175.

[25] CMS Collaboration, "Search for narrow resonances in dilepton mass spectra in proton-proton collisions at $\sqrt{s}$ = 13 TeV and combination with 8 TeV data", *Phys. Lett. B* **768** (2017) 57, doi:10.1016/j.physletb.2017.02.010, arXiv:1609.05391.

[26] D0 Collaboration, "Search for a heavy neutral gauge boson in the dielectron channel with 5.4 fb^{-1} of pp collisions at $\sqrt{s} = 1.96$ tev", *Physics Letters B* **695** (2011), no. 1, 88, doi:10.1016/j.physletb.2010.10.059.

[27] D0 Collaboration, "Search for additional neutral gauge bosons", *Physics Letters B* **385** (1996), no. 1, 471, doi:10.1016/0370-2693(96)00932-X.

[28] CDF Collaboration, "Search for high mass resonances decaying to muon pairs in $\sqrt{s} = 1.96$ tev pp collisions", *Phys. Rev. Lett.* **106** (Mar, 2011) 121801, doi:10.1103/PhysRevLett.106.121801, arXiv:1101.4578.

[29] P. Langacker, "The Physics of Heavy Z' Gauge Bosons", *Rev. Mod. Phys.* **81** (2009) 1199, doi:10.1103/RevModPhys.81.1199, arXiv:0801.1345.

[30] K. R. Lynch, E. H. Simmons, M. Narain, and S. Mrenna, "Finding Z' bosons coupled preferentially to the third family at LEP and the Tevatron", *Phys. Rev. D* **63** (2001) 035006, doi:10.1103/PhysRevD.63.035006, arXiv:hep-ph/0007286.

[31] CMS Collaboration, "The cms experiment at the cern lhc. the compact muon solenoid experiment", *Journal of Instrumentation* **3** (aug, 2008) S08004, doi:10.1088/1748-0221/3/08/S08004.

[32] CMS Collaboration, "Particle-flow reconstruction and global event description with the cms detector", *Journal of Instrumentation* **12** (2017), no. 10, P10003, doi:10.1088/1748-0221/12/10/p10003.

[33] CMS Collaboration, "Technical proposal for the Phase-II upgrade of the Compact Muon Solenoid", CMS Technical Proposal CERN-LHCC-2015-010, CMS-TDR-15-02, 2015.

[34] CMS Collaboration, "Performance of electron reconstruction and selection with the CMS detector in proton-proton collisions at $\sqrt{s} = 8$ TeV", *JINST* **10** (2015) P06005, doi:10.1088/1748-0221/10/06/P06005, arXiv:1502.02701.

[35] CMS Collaboration, "Performance of the cms muon detector and muon reconstruction with proton-proton collisions at $\sqrt{s} = 13$ tev", *Journal of Instrumentation* **13** (2018), no. 06, P06015, doi:10.1088/1748-0221/13/06/p06015.

[36] M. Cacciari, G. P. Salam, and G. Soyez, "The anti-k_{T} jet clustering algorithm", *JHEP* **04** (2008) 063, doi:10.1088/1126-6708/2008/04/063, arXiv:0802.1189.

[37] M. Cacciari, G. P. Salam, and G. Soyez, "Fastjet user manual", *Eur. Phys. J. C* **72** (2012) 1896, doi:10.1140/epjc/s10052-012-1896-2, arXiv:1111.6097.

[38] A. M. Sirunyan et al., "Performance of missing transverse momentum reconstruction in proton-proton collisions at $\sqrt{s} = 13$ TeV using the CMS detector", *Journal of Instrumentation* **14** (2019), no. 07, P07004, doi:10.1088/1748-0221/14/07/p07004.

[39] CMS Collaboration, "Jet algorithms performance in 13 TeV data", Technical Report CMS-PAS-JME-16-003, CERN, Geneva, 2017.

[40] A. M. Sirunyan et al., "Identification of heavy-flavour jets with the CMS detector in pp collisions at 13 TeV", *Journal of Instrumentation* **13** (2018), no. 05, P05011, doi:10.1088/1748-0221/13/05/p05011.

[41] CMS Collaboration, "Performance of reconstruction and identification of τ leptons decaying to hadrons and ν_τ in pp collisions at $\sqrt{s} = 13$ TeV", *JINST* **13** (2018), no. 10, P10005, doi:10.1088/1748-0221/13/10/P10005, arXiv:1809.02816.

[42] CMS Collaboration, "Identification of hadronic tau lepton decays using a deep neural network", *JINST* **17** (2022) P07023, doi:10.1088/1748-0221/17/07/P07023, arXiv:2201.08458.

[43] M. Pioppi, "Tau reconstruction and identification with particle-flow techniques using the cms detector at lhc", *Nuclear Physics B - Proceedings Supplements* **189** (2009) 311, doi:10.1016/j.nuclphysbps.2009.03.051. Proceedings of the Tenth International Workshop on Tau Lepton Physics.

[44] CMS Collaboration, "Search for dark matter and supersymmetry with a compressed mass spectrum in the vector boson fusion topology in proton-proton collisions at $\sqrt{s} = 8$ TeV", *Phys. Rev. Lett.* **118** (2017) 021802, doi:10.1103/PhysRevLett.118.021802, arXiv:1605.09305.

[45] A. Flórez et al., "Anapole dark matter via vector boson fusion processes at the LHC", *Phys. Rev. D* **100** (2019) 016017, doi:10.1103/PhysRevD.100.016017, arXiv:1902.01488.

[46] CMS Collaboration, "The CMS trigger system", *JINST* **12** (2017) P01020, doi:10.1088/1748-0221/12/01/P01020, arXiv:1609.02366.

[47] J. Alwall et al., "The automated computation of tree-level and next-to-leading order differential cross sections, and their matching to parton shower simulations", *JHEP* **07** (2014) 079, doi:10.1007/JHEP07(2014)079, arXiv:1405.0301.

[48] S. Alioli, P. Nason, C. Oleari, and E. Re, "A general framework for implementing NLO calculations in shower Monte Carlo programs: the POWHEG BOX", *JHEP* **06** (2010) 043, doi:10.1007/JHEP06(2010)043, arXiv:1002.2581.

[49] T. Sjöstrand et al., "An introduction to pythia 8.2", *Computer Physics Communications* **191** (2015) 159, doi:10.1016/j.cpc.2015.01.024.

[50] A. Flórez et al., "Searching for new heavy neutral gauge bosons using vector boson fusion processes at the lhc", *Physics Letters B* **767** (2017) 126, doi:10.1016/j.physletb.2017.01.062.

[51] CMS Collaboration, "Event generator tunes obtained from underlying event and multiparton scattering measurements", *Eur. Phys. J. C* **76** (2016) 155, doi:10.1140/epjc/s10052-016-3988-x, arXiv:1512.00815.

[52] CMS Collaboration, "Extraction and validation of a new set of CMS PYTHIA8 tunes from underlying-event measurements", *Eur. Phys. J. C* **80** (2020) 4, doi:10.1140/epjc/s10052-019-7499-4, arXiv:1903.12179.

[53] NNPDF Collaboration, "Parton distributions for the LHC run II", *JHEP* **04** (2015) 040, doi:10.1007/JHEP04(2015)040, arXiv:1410.8849.

[54] G. Collaboration, "GEANT4– simulation toolkit", *Nuclear Instruments and Methods in Physics Research Section A: Accelerators, Spectrometers, Detectors and Associated Equipment* **506** (2003), no. 3, 250, doi:10.1016/S0168-9002(03)01368-8.

[55] CMS Collaboration, "Precision luminosity measurement in proton-proton collisions at $\sqrt{s} = 13$ TeV in 2015 and 2016 at CMS", *Eur. Phys. J. C* **81** (2021) 800, doi:10.1140/epjc/s10052-021-09538-2, arXiv:2104.01927.

[56] CMS Collaboration, "CMS luminosity measurement for the 2017 data-taking period at $\sqrt{s}$ = 13 TeV", CMS Physics Analysis Summary CMS-PAS-LUM-17-004, 2018.

[57] CMS Collaboration, "CMS luminosity measurement for the 2018 data-taking period at $\sqrt{s}$ = 13 TeV", CMS Physics Analysis Summary CMS-PAS-LUM-18-002, 2019.

[58] CMS Collaboration, "Performance of the CMS muon detector and muon reconstruction with proton-proton collisions at $\sqrt{s} = 13$ TeV", *JINST* **13** (2018) P06015, doi:10.1088/1748-0221/13/06/P06015, arXiv:1804.04528.

[59] CMS Collaboration, "Measurement of the inclusive W and Z production cross sections in pp collisions at $\sqrt{s} = 7$ TeV", *JHEP* **10** (2011) 132, doi:10.1007/JHEP10(2011)132, arXiv:1107.4789.

[60] J. Butterworth et al., "PDF4LHC recommendations for LHC Run II", *J. Phys. G* **43** (2016) 023001, doi:10.1088/0954-3899/43/2/023001, arXiv:1510.03865.

[61] P. M. Nadolsky et al., "Implications of CTEQ global analysis for collider observables", *Phys. Rev. D* **78** (2008) 013004, doi:10.1103/PhysRevD.78.013004, arXiv:0802.0007.

[62] A. D. Martin, W. J. Stirling, R. S. Thorne, and G. Watt, "Update of parton distributions at NNLO", *Phys. Lett. B* **652** (2007) 292, doi:10.1016/j.physletb.2007.07.040, arXiv:0706.0459.

[63] M. Ubiali, "NNPDF1.0 parton set for the LHC", *Nucl. Phys. Proc. Suppl.* **186** (2009) 62, doi:10.1016/j.nuclphysbps.2008.12.020, arXiv:0809.3716.

[64] G. Cowan, K. Cranmer, E. Gross, and O. Vitells, "Asymptotic formulae for likelihood-based tests of new physics", *Eur. Phys. J. C* **71** (2011) 1554, doi:10.1140/epjc/s10052-011-1554-0, arXiv:1007.1727. [Erratum: doi:10.1140/epjc/s10052-013-2501-z].

[65] T. Junk, "Confidence level computation for combining searches with small statistics", *Nucl. Instrum. Meth. A* **434** (1999) 435, doi:10.1016/S0168-9002(99)00498-2.

[66] A. L. Read, "Presentation of search results: the CL_s technique", *J. Phys. G* **28** (2002) 2693, doi:10.1088/0954-3899/28/10/313.

[67] CMS Collaboration, "The CMS statistical analysis and combination tool: COMBINE", 2024. arXiv:2404.06614. Submitted to *Comput. Softw. Big Sci.*

[68] Belle Collaboration, "Measurement of the τ lepton polarization and $R(D^*)$ in the decay $\bar{B} \to D^* \tau^- \bar{\nu}_\tau$ with one-prong hadronic τ decays at Belle", *Phys. Rev. D* **97** (2018) 012004, doi:10.1103/PhysRevD.97.012004, arXiv:1709.00129.

[69] Belle Collaboration, "Measurement of the branching ratio of $\bar{B}^0 \to D^{*+} \tau^- \bar{\nu}_\tau$ relative to $\bar{B}^0 \to D^{*+} \ell^- \bar{\nu}_\ell$ decays with a semileptonic tagging method", *Phys. Rev. D* **94** (2016) 072007, doi:10.1103/PhysRevD.94.072007, arXiv:1607.07923.

[70] Belle Collaboration, "Measurement of the τ lepton polarization and $R(D^*)$ in the decay $\bar{B} \to D^* \tau^- \bar{\nu}_\tau$", *Phys. Rev. Lett.* **118** (2017) 211801, doi:10.1103/PhysRevLett.118.211801, arXiv:1612.00529.

[71] Belle Collaboration, "Measurement of the branching ratio of $\bar{B} \to D^{(*)} \tau^- \bar{\nu}_\tau$ relative to $\bar{B} \to D^{(*)} \ell^- \bar{\nu}_\ell$ decays with hadronic tagging at Belle", *Phys. Rev. D* **92** (2015) 072014, doi:10.1103/PhysRevD.92.072014, arXiv:1507.03233.

[72] LHCb Collaboration, "Measurement of the ratio of the $B^0 \to D^{*-} \tau^+ \nu_\tau$ and $B^0 \to D^{*-} \mu^+ \nu_\mu$ branching fractions using three-prong τ-lepton decays", *Phys. Rev. Lett.* **120** (2018) 171802, doi:10.1103/PhysRevLett.120.171802, arXiv:1708.08856.

[73] LHCb Collaboration, "Measurement of the ratio of branching fractions $\mathcal{B}(\bar{B}^0 \to D^{*+} \tau^- \bar{\nu}_\tau) / \mathcal{B}(\bar{B}^0 \to D^{*+} \mu^- \bar{\nu}_\mu)$", *Phys. Rev. Lett.* **115** (2015) 111803, doi:10.1103/PhysRevLett.115.111803, arXiv:1506.08614. [Erratum: Phys.Rev.Lett. 115, 159901 (2015)].

[74] M. Abdullah et al., "Probing a simplified, W' model of $R(D^{(*)})$ anomalies using b-tags, τ leptons and missing energy", *Phys. Rev. D* **98** (2018), no. 5, 055016, doi:10.1103/PhysRevD.98.055016, arXiv:1805.01869.

[75] A. Flórez et al., "On the sensitivity reach of LQ production with preferential couplings to third generation fermions at the LHC", *Eur. Phys. J. C* **83** (2023), no. 11, 1023, doi:10.1140/epjc/s10052-023-12177-4, arXiv:2307.11070.